

## Long-range correlations in the electric signals that precede rupture

P. A. Varotsos,\* N. V. Sarlis, and E. S. Skordas

*Solid State Section, Physics Department, University of Athens Panepistimiopolis, Zografos, Athens 157 84, Greece*

(Received 10 March 2002; published 12 July 2002)

The Smoluchowski-Chapman-Kolmogorov functional equation is applied to the electric signals that precede rupture. The results suggest a non-Markovian character of the analyzed data. The rescaled range Hurst and detrended fluctuation analyses, as well as that related with the “mean distance a walker spanned,” lead to power-law exponents, which are consistent with the existence of long-range correlations. A “universality” in the power spectrum characteristics of these signals emerges, if an analysis is made (not in the conventional time frame, but) in the “natural” time domain. Within this frame, it seems that certain power spectrum characteristics of ion current fluctuations in membrane channels distinguish them from the electric signals preceding rupture. The latter exhibit a behavior compatible with that expected from a model based on the random field Ising Hamiltonian at the critical point.

DOI: 10.1103/PhysRevE.66.011902

PACS number(s): 87.17.-d, 05.40.-a

### I. INTRODUCTION

Traditionally, processes are characterized by assuming that correlations decay exponentially. However, it is well known (e.g., see Refs. [1,2]) that there is one major exception: at the critical point, the exponential decay turns into a power-law decay.

Long range power-law correlations have been found in a wide variety of systems [1,2]. As soon as power-law correlations are found, they are usually quantified with a “critical” exponent.

We recall that a stochastic process  $X(t)$  is called self-similar with index  $H$  if it has the property  $X(\lambda t) = \lambda^H X(t)$ , where the equality concerns the finite-dimensional distributions of the process  $X(t)$  on the right- and the left-hand side of the equation (not the values of the process). Having a time series of stationary increments one can study correlations in a self-similar time series applying the statistical tools to a random walk given by the cumulative time series. For the conventional one-dimensional random walk model, a walker moves either “up” [ $u(i) = +1$ ] or “down” [ $u(i) = -1$ ] one unit length for each step of the walk. The question, which is usually asked [3,4], is whether a “walk” displays only short-range correlations (as in an  $n$ -step Markov chain) or long-range correlations (as in critical phenomena and other scale-free “fractal” phenomena). The statistical quantity usually treated in any walk (e.g., see Ref. [5]) is the root-mean-square fluctuation  $F(l)$  about the average of the displacement of a quantity  $\Delta y(l)$ , which is defined by  $\Delta y(l) = y(l_0 + l) - y(l_0)$ , where  $y(l) \equiv \sum_{i=1}^l u(i)$ . This is described by a power law [3,4]

$$F(l) \sim l^\alpha \quad (1)$$

with  $\alpha \neq 1/2$  if there is no characteristic length (i.e., if the correlations between  $u(i)$  and  $u(j)$  are power-law long-range correlations). We recall that the case  $\alpha = 1/2$  represents the absence of long-range correlations (e.g., see pp. 117–119

of Ref. [6]). Thus, in a double logarithmic plot, the value of the slope  $\alpha$ , resulting from a least-squares fit to a straight line, reveals the presence, or not, of long-range correlations.

In Refs. [3,4], for example, the reasons why conventional scaling analyses cannot be applied reliably to an entire DNA sequence (but only to subsequences) have been summarized. To overcome the difficulty, a method had been developed [7,8], termed detrended fluctuation analysis (DFA), which is specifically adapted to handle problems associated with non-stationary sequences. It is one of the basic aims of the present paper to apply this well established method to the case of electric signals that precede rupture. As an example, we consider the so-called seismic electric signals (SES), which are low frequency ( $\leq 1$  Hz) changes of the electric field of the earth that have been found in Greece [9,10] and Japan [11] to precede earthquakes, with a lead time from several hours to a few months [9–13]; the relevant process has a finite variance [10,11,13].

Beyond DFA, we also apply here to SES the rescaled range Hurst analysis [14,15] as well as that related with the “mean distance a walker spanned” [16,17]. The first two methods, between others, have been recently used by Mercik and Weron [18] to study the stochastic origins of the long-range correlations of ionic current fluctuations in membrane channels (ICFMC). We clarify that (see Ref. [19] and references therein) single ionic channels in a membrane open and close spontaneously in a stochastic way, resulting in current and voltage changes, which resemble the realizations of random telegraph signals, RTS (dichotomous noise). It has been shown [20] that the action of membrane-embedded enzymes depends critically on fluctuations of the membrane potential, and that the main source of these fluctuations originates in the fluctuations of ionic concentrations due to the action of ion channels. Note that the SES activities have also an RTS feature, which, as noticed elsewhere [12,21], could be understood in the context of dynamic phase transitions. As an example, Fig. 1 depicts an excerpt of the SES activity recorded on April 18, 1995 (cf. the full record can be found in Ref. [13]), that preceded the earthquake with magnitude 6.6 that occurred at Grevena-Kozani on May 13, 1995. This lasted

\*Electronic address: pvaro@otenet.gr

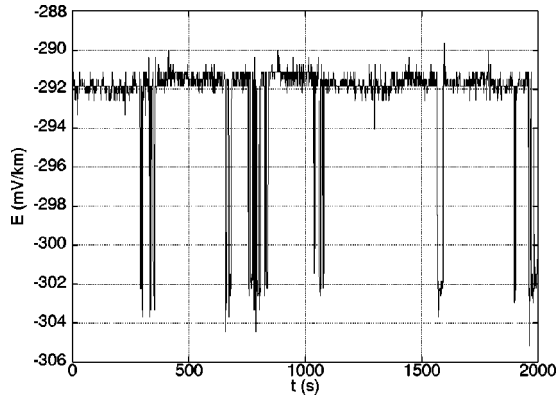


FIG. 1. Excerpt of an SES activity, which was recorded on April 18, 1995 with a sampling frequency  $f_{exp}=1$  sample/sec. The electric field  $E$  is measured in mV/km.

for around three and a half hours and was collected with a sampling rate  $f_{exp}=1$  sample/sec (thus we have  $N=11\,900$  data points).

The present paper is organized as follows: In Sec. II, we investigate the stationarity of the aforementioned SES activity, by using the notion of the quantiles introduced by Weron and coworkers (see Ref. [18] and references therein). The non-Markovian character of this signal is shown in Sec. III by using the Smoluchowski-Chapman-Kolmogorov equation. The Hurst, DFA, and the “mean distance a walker spanned” analyses of the aforementioned example of SES activity are presented in Secs. IV, V, and VI, respectively. Section VII is reserved for the analysis in the “natural time” domain (explained in detail in Ref. [22]), of both data sets, i.e., SES activities and ICFMC. The conclusions are summarized in Sec. VIII.

## II. THE STATIONARITY OF THE SIGNAL

This was studied, as mentioned, by using the notion of quantiles [18]. A quantile of order  $\epsilon \in (0,1]$  is such a value  $k_\epsilon(t)$  that the probability of the recorded signal being less than  $k_\epsilon$  at the moment  $t$  is equal to  $\epsilon$ . Following the procedure of Ref. [18], we cut the whole record into smaller sub-records (of length 100 s), and the resulting quantiles are shown in Fig. 2. Since these lines are parallel to the time axis (time invariant), we may assume [18] that the investigated time series is stationary and has constant mean and variance within the examined limits. We clarify that the stationarity indicated by quantile lines can be proved mathematically (see Ref. [18] and references therein); stationarity can be easily observed in a large time scale although locally the time series seems to be nonstationary.

## III. TEST OF MARKOVIANITY

In order to test the Markovianity of an SES activity, we use the Smoluchowski-Chapman-Kolmogorov functional equation, which presents the most basic test of Markovian character of finite stochastic chains. This has been used by Fuliński *et al.* [19] in the relevant study of the ICFMC.

Following Ref. [19], we consider a stochastic process  $\xi(t)$

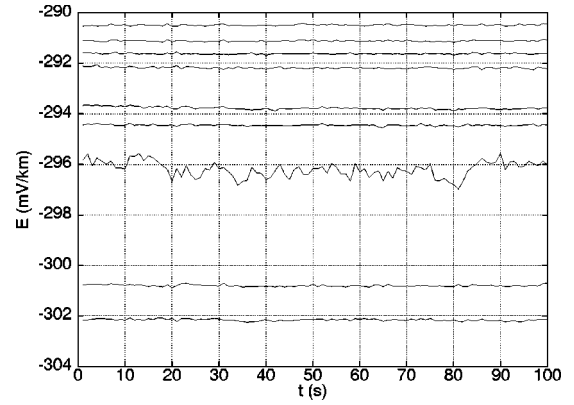


FIG. 2. The quantile lines  $k_\epsilon(t)$  of the SES activity on April 18, 1995. The quantiles  $k_\epsilon$  are of order from  $\epsilon=0.1$  to  $0.9$  step  $0.1$  counting from the bottom to the top of the figure.

over  $M$  discrete states:  $\xi(t) \in \{\xi_1, \xi_2, \dots, \xi_M\}$ . These states in the present case of SES activity denote the values of the electric field  $m\delta E < E_m < (m+1)\delta E$ ,  $m=0, \dots, M-1$ , and the stochastic process is the measured time series  $\xi(t) = E(t)$ . Let  $P_k(\xi_\alpha, t_1; \dots; \xi_\gamma, t_k)$  ( $\alpha, \beta, \gamma, \dots = 1, \dots, M$ ) be the probability that the process  $\xi(t)$  is in the state  $\xi_\alpha$  at time  $t_1, \dots$  and in the state  $\xi_\gamma$  at time  $t_k$ . After defining the conditional probability

$$P_{1|k}(\xi_\alpha, t_1 | \xi_\beta, t_2; \dots; \xi_\gamma, t_k + 1) = \frac{P_{k+1}(\xi_\alpha, t_1; \xi_\beta, t_2 \dots; \xi_\gamma, t_k + 1)}{P_k(\xi_\beta, t_2 \dots; \xi_\gamma, t_k + 1)}, \quad (2)$$

the Markovianity of the process  $\xi(t)$  is defined by

$$P_{1|n}(\xi_\alpha, t | \xi_\beta, t_1; \dots; \xi_\gamma, t_n) = P_{1|1}(\xi_\alpha, t | \xi_\beta, t_1), \forall t > t_1 > \dots > t_n. \quad (3)$$

The so-called Smoluchowski-Chapman-Kolmogorov (SCK) functional equation,

$$P_{1|1}(\xi_\alpha, t | \xi_\gamma, t_2) = \sum_{\xi_\beta = \xi_1}^{\xi_M} P_{1|1}(\xi_\alpha, t | \xi_\beta, t_1) P_{1|1}(\xi_\beta, t_1 | \xi_\gamma, t_2) \quad \forall t > t_1 > t_2, \quad (4)$$

results from the definitions (2) and (3), and from the standard properties of probability distributions (see Ref. [19] and references therein). The stochastic process  $\xi(t)$ , which does not satisfy either the basic definition, Eq. (3) or the SCK Eq. (4) is not Markovian.

The corresponding experimental electric field probability density function (PDF) (obtained in a way similar to that followed by Mercik *et al.* [18], in their Fig. 2) reveals a bimodal feature (with finite variation and standard deviation), which is evident in Fig. 1. The two states probabilities  $P_2(m, t; n, 0) \equiv P_2(m, t_1; n, t_2)$ , with  $m, n=1, 2$ , (1: upper level, 2: lower level),  $t=t_1-t_2$  (stationary process, see Sec. II), were calculated in a way similar to that followed for

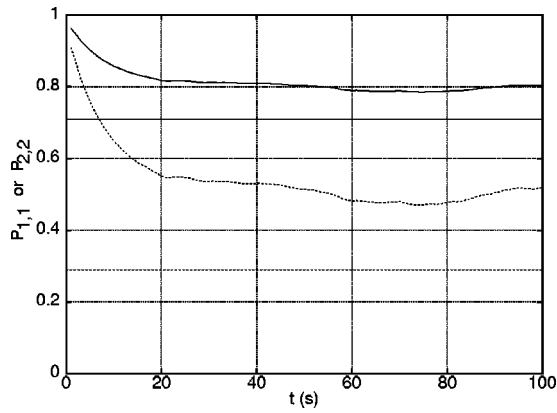


FIG. 3. Field-field conditional probabilities  $P_{1,1}(t)$  (solid curve) and  $P_{2,2}(t)$  (dotted curve) for the RTS (dichotomous) representation ( $M=2$ ) of the SES activity mentioned in Fig. 1. The solid and dotted straight lines depict, respectively, the  $P_1(1)$  and  $P_1(2)$  for randomly generated data (Markov process).

finding stationary probabilities  $P_1(m)$ , i.e., by counting [19] the relative numbers of pairs of states separated by time interval  $t$ , such that  $E(t_1) \in$  state  $m$ , and  $E(t_2) \in$  state  $n$ . Thus, the field-field conditional probabilities  $P_{m,n}(t) \equiv P_{1|1}(m, t_1 | n, t_2)$  were determined from  $P_{m,n}(t) = P_2(m, t; n, 0) / P_1(n)$ . The results for  $P_{1,1}(t)$  and  $P_{2,2}(t)$  are shown in Fig. 3, along with straight lines  $P_1(1)$  and  $P_1(2)$ ; the latter two correspond to randomly generated Markovian RTS (dichotomous) series (control data) and the relevant volatility, given by Ref. [23]  $P_1(1 - P_1)/N$ , results less than  $10^{-3}$ . If  $D_{1,1}(t)$  denotes the difference between the left- and right-hand sides of the SCK Eq. (4) (for a time shift 1 s), the corresponding function calculated from the functions depicted in Fig. 3, is presented in Fig. 4. An inspection of the latter figure shows that the deviations from the SCK relation for the experimental SES series (upper curve) are drastically larger than those for the control Markovian series (bottom curve). Such a result suggests [19] the non-Markovian character of the analyzed data.

#### IV. HURST ANALYSIS

A way of studying correlations in a time series is provided by the Hurst analysis [14] known as rescaled range analysis

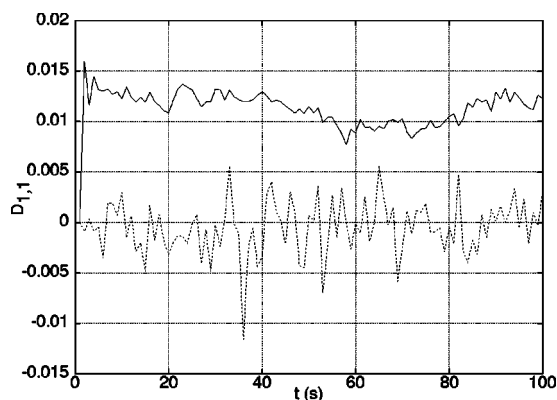


FIG. 4. The deviation  $D_{1,1}(t)$  from the SCK relation. Upper curve: experimental SES time series mentioned in Fig. 1; bottom curve: randomly generated data (Markov process).

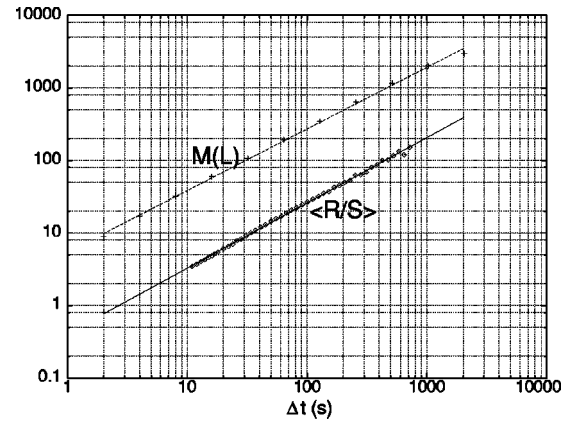


FIG. 5. The rescaled range analysis  $\langle R/S \rangle$  (diamonds, the lower line) as a function of the time-lag  $\Delta t$  (log-log plot) for the SES activity mentioned in Fig. 1; the slope of this straight line leads to the Hurst exponent  $H$ . The upper line (crosses) corresponds to  $M(L)$  (in mV/km) and its slope leads to the exponent  $\alpha'$  (see the text).

( $R/S$ ). This compares the correlations in the time series measured at different time scales. The results of such an analysis are given in the lower curve of Fig. 5. The value of the Hurst exponent  $H$  is found to be  $H = 0.86 \pm 0.09$ . (The errors mainly come from the uncertainty in fitting either the original signal or the dichotomous one.) This is far from the value  $H = 1/2$ , which suggests that the changes in the values of a time series are purely random (and hence uncorrelated with each of other). Recall that, when  $1/2 < H < 1$  (which is our case), the time series is called persistent and it has a long memory property, e.g., see Ref. [15] (in this case the increase in the values of a series is more likely to be followed by an increase, and conversely, the decrease is more likely to be followed by a decrease). The fractal dimension  $d$  is found from the relation  $d = 2 - H$  which, after considering the aforementioned  $H$  value, leads to  $d = 1.14 \pm 0.09$ .

#### V. DETRENDED FLUCTUATION ANALYSIS (DFA)

Advantages of DFA over conventional methods (e.g., spectral analysis and Hurst analysis) are that it permits the detection of intrinsic self-similarity embedded in a seemingly nonstationary time series, and also avoids the spurious detection of apparent self-similarity, which may be an artifact of extrinsic trends [7,8,3,4]. A recent investigation of the question of whether DFA does provide insight in the long-time behavior that goes beyond the possibilities of spectral analysis has been discussed in detail in Ref. [24].

We first divide a series of length  $N$  into  $N/l$  nonoverlapping fragments, each of  $l$  observations, and determine a local trend of the subseries. Next we define the detrended process in every fragment denoted by  $y_d(n)$  as the difference between the original value of the series and the local trend. If the time series was recorded with the frequency  $f_{exp}$ , we calculate the mean variance of the detrended process  $F_d^2(l)$ ,

$$F_d^2(\Delta t) = \frac{1}{N} \sum_{l=1}^{N/l} \sum_{n=1}^l y_d^2(n), \quad (5)$$

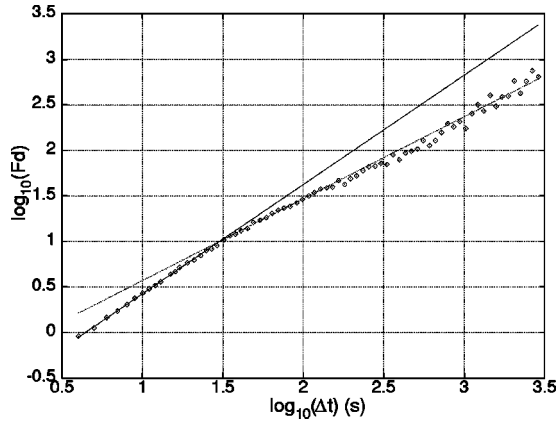


FIG. 6. The dependence of  $F_d$  (in mV/km) on the time-lag  $\Delta t$  in the DFA of the SES activity mentioned in Fig. 1.

where  $\Delta t = l/f_{exp}$ . The results obtained by such a procedure [25] for the aforementioned SES activity are depicted in Fig. 6. The slope of this log-log plot (after making a least-squares fit to a single straight line) leads to the value  $\alpha \approx 0.95 \pm 0.01$  (the estimation error becomes  $\pm 0.04$  upon disregarding points related with either  $\Delta t \leq 10$  s and/or  $\Delta t \geq 200$  s). This reveals long-range correlations, as mentioned above in the discussion of Eq. (1). Note that if, alternatively [26], we fit the data with two straight lines (which are depicted in Fig. 6) the corresponding values are  $\alpha \approx 1.19 \pm 0.02$  and  $\alpha \approx 0.88 \pm 0.02$  for the short times and long times (i.e., smaller than around 30 s and larger than  $\sim 30$  s) respectively. The power spectrum exponent  $S(f) \sim 1/f^\beta$  is found from the relation [8]  $\beta = 2\alpha - 1$ , thus we obtain  $\beta \approx 1.4$  and  $\beta \approx 0.8$ , respectively. The two scaling regions can be interpreted as indicating the presence of two different interactions: short time interactions, for  $t \leq 30$  s, which are very strong, and long-range interactions, a little weaker and persistent. Note that Antal *et al.* [27] recently studied the PDF of the roughness, i.e., of the temporal variance, of  $1/f^\beta$  noise signals. They suggest that for  $\beta \leq 1/2$  the scaled PDFs in both periodic and the nonperiodic cases are Gaussian, but for  $\beta > 1/2$  they differ from the Gaussian and from each other; both deviations increase with growing  $\alpha$ .

**VI. THE EXPONENT FROM THE “MEAN DISTANCE A WALKER SPANNED”**

The time series can be analyzed using the quantity  $M(L)$ , the mean distance a walker spanned [16,28,17] within time  $L$ . If we denote

$$W(j) = \sum_{t=1}^j [X(t) - X_{ave}], \tag{6}$$

we get

$$M(L) = \langle |W(j) - W(j+L)| \rangle_j, \tag{7}$$

where  $X_{ave}$  corresponds to the average over the whole time series,  $j = 1, \dots, N-L$ , and  $\langle \rangle_j$  denotes the average over  $j$ . From a physics viewpoint, the quantity  $M(L)$  may be re-

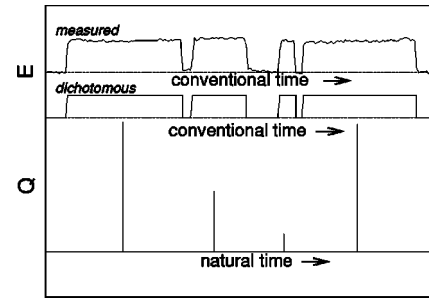


FIG. 7. How a dichotomous series of pulses can be read in “natural time”; the latter serves as an index of the occurrence of each pulse (reduced by the total number of pulses), while the amplitude is proportional to the duration of each electric pulse.

garded as the variance evolution of a random walker’s total displacement mapped from the time series  $X(t)$ . From the slope of the log-log plot of  $M(L)$  versus  $L$ , upon considering the relation  $M(L) \propto L^{\alpha'}$ , we can determine  $\alpha'$ . Such an analysis leads to the upper straight line of Fig. 5, which gives  $\alpha' = 0.87 \pm 0.12$ . This value also suggests long-range correlations.

**VII. ANALYSIS IN THE “NATURAL TIME” DOMAIN**

The *natural time*  $\chi$  serves as an index for the occurrence of an event (reduced by the total number of events, thus being smaller than, or equal to, unity) [22]. Let us, therefore, denote by  $Q_k$  the duration of the  $k$ th transient pulse of the dichotomous series of an SES activity comprised of  $K$  pulses (Fig. 7). The natural time  $\chi$  is introduced by ascribing to this pulse the value  $\chi_k = k/K$ . If we now consider the evolution  $(\chi_k, Q_k)$ , we can define the continuous function  $F(\omega)$  (this should not be confused with the discrete Fourier transform).

$$F(\omega) = \sum_{k=1}^K Q_k \exp\left(i\omega \frac{k}{K}\right), \tag{8}$$

where  $\omega = 2\pi\phi$ . Since the quantity  $\phi (\equiv \omega/2\pi)$  is related with the natural time, it is termed *natural frequency*. We normalize  $F(\omega)$  by dividing it by  $F(0)$ ,

$$\Phi(\omega) = \frac{\sum_{k=1}^K Q_k \exp\left(i\omega \frac{k}{K}\right)}{\sum_{k=1}^K Q_k} = \sum_{k=1}^N p_k \exp\left(i\omega \frac{k}{K}\right), \tag{9}$$

where  $p_k = Q_k / \sum_{n=1}^K Q_n$ . Thus, the quantities  $p_k$  describe a “probability” to observe the transient at natural time  $\chi_k$ . From Eq. (9), we can obtain the normalized power spectrum  $\Pi(\omega) = |\Phi(\omega)|^2$ . For natural frequencies  $\phi$  less than 0.5,  $\Pi(\omega)$  or  $\Pi(\phi)$  reduce to a characteristic function for the probability distribution  $p_k$  in the context of probability theory. The procedure of reading a series of electric pulses in the natural time domain is depicted in Fig. 7. We now apply this procedure to the SES activities related [10,29] to the three strongest earthquakes that occurred in Greece since

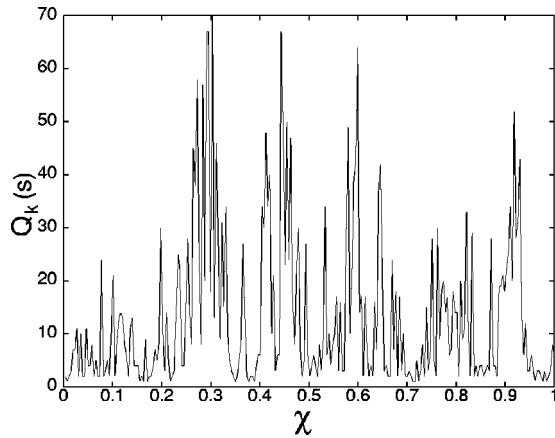


FIG. 8. The SES activity mentioned in Fig. 1 read in “natural time.”

1988, i.e., on May 13, 1995 (with magnitude  $M=6.6$ ), June 15, 1995 ( $M=6.5$ ), and July 26, 2001 ( $M=6.6$ ). Once an SES activity has been recorded, we can read it in the natural time domain (for example, see Fig. 8 for the SES activity mentioned in Fig. 1) and then proceed to its analysis. The same type of analysis was applied to the ICFMC data reported in Ref. [19] and subsequently analyzed in Refs. [18,26,30,31]. Figure 9 depicts  $\Pi(\phi)$  for the SES activities along with that corresponding to the dichotomous signal of the ICFMC data studied in Refs. [18,30]. An inspection of this figure shows the following three facts: First, for *natural frequencies* smaller than 0.5 (see the inset of Fig. 9), the curves labeled “SES activities,” which correspond to the  $\Pi(\phi)$  values of the SES activities, scatter around the solid curve that has been theoretically estimated (see the Appendix). We emphasize that this occurs only if we consider the totality of the SES activity, and we do not, e.g., omit a significant portion of its initiation. Second, the curves related to the SES activities cross at a point with a  $\phi$  value very close to unity, i.e.,  $\phi \approx 1.05$ . How this point is approached can be

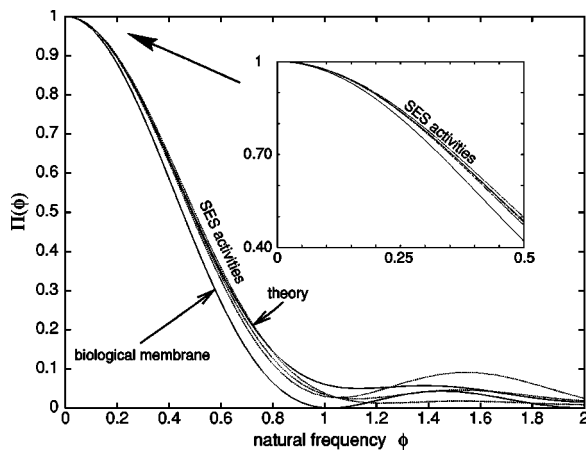


FIG. 9. The normalized power spectra  $\Pi(\phi)$  for the three SES activities (dotted lines) mentioned in the text along with that of the ICFMC (labeled biological membrane, lower solid curve). The upper solid curve corresponds to the theoretical estimation discussed in the Appendix.

studied by means of the so-called  $\beta$ -function (see p. 288 of Ref. [32]) when following a procedure similar to that discussed in Ref. [33]. Third, in the region  $0 \leq \phi \leq 1$ , the solid line related with the ICFMC seems to lie (not far from, but) systematically lower than those of the SES activities (see also the Appendix).

## VIII. CONCLUSIONS

Using methods of statistical physics, we found that SES activities exhibit long-range correlations (memory). Specifically, when applying a test based on the Smoluchowski-Chapman-Kolmogorov functional equation, the results suggest the non-Markovian character of the SES data. The quantiles procedure was used for the study of the stationarity of the signal. The rescaled range Hurst and detrended fluctuation analyses led to power-law exponents that indicate long-range correlations. This result was also confirmed by means of the exponent resulted from the analysis of the “mean distance a walker spanned.” Furthermore, the “natural” time domain analysis was applied to the SES activities as well as to the ICFMC. Within such a frame, the following two main conclusions hold for certain power spectrum characteristics of the SES activities, namely, their  $\Pi(\phi)$  values versus  $\phi$ : First, they lie above those of the ICFMC in the region  $0 \leq \phi \leq 1$ . Second, in the range  $0 \leq \phi \leq 0.5$ , they are compatible with those calculated (see the Appendix) when adopting a model to describe criticality.

## ACKNOWLEDGMENTS

We express our sincere thanks to Professor K. Weron and Dr. S. Mercik for sending us a lot of useful information on their work as well as for making several fruitful suggestions. Furthermore, we thank Professor P.N.R. Usherwood and Dr. I. Mellor for providing us with the experimental data of ion current through high-conductance locust potential channel. We also gratefully acknowledge several stimulating discussions with Professor E. Manousakis.

## APPENDIX: THE NATURAL POWER SPECTRUM OF SES ACTIVITIES

The Taylor expansion of  $\Pi(\omega)$  reveals that

$$\Pi(\omega) = 1 - \kappa_1 \omega^2 + \kappa_2 \omega^4 + \kappa_3 \omega^6 + \kappa_4 \omega^8 + \dots, \quad (\text{A1})$$

where  $\kappa_1 = \langle \chi^2 \rangle - \langle \chi \rangle^2$  is the variance of  $\chi$ , and  $\langle \chi^n \rangle = \sum_{k=1}^N (\chi_k)^n p_k$  are the moments of the distribution of  $\chi$ . The most useful quantity around  $\omega=0$  is the variance  $\kappa_1$  of the natural time distribution. This is so, because the various normalized power spectra (in Fig. 9) are grouped together as  $\omega$  or  $\phi$  tend to 0 depending on their  $\kappa_1$  values. The value of  $\kappa_1$  that reproduces the ICFMC data is  $0.080 \pm 0.003$ , while for the SES activities is  $0.070 \pm 0.005$ .

Indentation experiments even in simple ionic crystals showed that electric signals are emitted, without the action of any external electric field, due to (formation and motion of) point and linear defects [34]. Independent laboratory measurements [35] revealed that, as the glass transition is ap-

proached, a polarization time series is emitted which arises from the reorientation process of electric dipoles; this process includes a large number of atoms (cooperativity). A comparison shows that the feature of the latter time series is strikingly similar [12] to the measured SES activities. This similarity is reminiscent of the pressure stimulated currents model [6], which suggests that, upon a gradual variation of the pressure (stress)  $P$  on a solid, transient electric signals are emitted, from the (re)orientation of electric dipoles (formed due to disorder), when approaching a *critical* pressure (stress)  $P_{cr}$  obeying the condition  $(dP/dt)_T v^m/kT = -1/\tau(P_{cr})$ , where  $v^m$  is the migration volume, defined as  $v^m = (\partial g^m/\partial P)_T$ ,  $g^m$  being the Gibbs migration energy and  $\tau(P_{cr})$  the relaxation time for the (re)orientation process. The values of  $v^m$  associated with SES generation should exceed the mean atomic volume by orders of magnitude, and this entails that the relevant (re)orientation process should involve the motion of a large number of “atoms” (see p. 404 of Ref. [6]). Thus, the laboratory measurements [35] fortify the suggestion [6,12] that the emission of the SES activities could be discussed in the frame of the theory of *dynamic phase transitions*. The very stochastic nature of the relaxation process has been repeatedly discussed in the literature (see p. 350 of Ref. [36] and references therein; other suggestions have been reviewed in Ref. [37], while recent illuminating aspects have been forwarded in Ref. [38]). A stochastic analysis was based on the concept of clusters, the structural rearrangement of which develops in time [36]. According to this analysis the exponential relaxation of the polarization is arrested at a random time variable  $\eta_i$  and the instantaneous orientation reached at this instant is “frozen” at a value  $\exp(-\beta_i \eta_i)$  where  $\beta_i = b = \text{const}$  (see Fig. 11.19 of Ref. [36]). Assuming that  $\eta_i$  itself follows an exponential distribution, with a time constant  $\tau_0 \ll \tau \equiv \tau(P_{cr})$ , an almost constant current would be expected for as long as this unit

“lives” (i.e., for a duration  $\eta_i$ ).

The RTS feature of an SES activity might be understood in the following context: The duration  $Q$  of a pulse is just the sum of  $n$  such identical units  $Q = \sum_{i=1}^n \eta_i$ . Under this assumption, the duration  $Q_k$  of the  $k$ th pulse, in an SES activity, follows the gamma distribution with a mean lifetime  $n_k \tau_0$  and variance  $n_k \tau_0^2$  (e.g., see Lemma 8.1.6.5. of Ref. [39]); here  $n_k$  is the number of exponential lifetime backup units that act cooperatively. If at the critical point,  $n_k$  backup units were available at the  $k$ th current emission, then the average number of backup units for the  $k+1$  emission would be the same. This assumption is reminiscent of the aspect that the reorientation of a spin, in the random-field Ising Hamiltonian, will cause on average one more spin to flip at the critical point [40]. Under these assumptions, one finally obtains [22]

$$\Pi(\omega) = \frac{18}{5\omega^2} - \frac{6 \cos \omega}{5\omega^2} - \frac{12 \sin \omega}{5\omega^3}. \quad (\text{A2})$$

Expanding Eq. (A2) around  $\omega=0$ , we find  $\kappa_1=0.070$ . An inspection of the inset of Fig. 9 shows that, for the region of natural frequencies  $0 \leq \phi \leq 0.5$ , where  $\Pi(\phi)$  should be considered as a characteristic function for  $p_k$ , the experimental results for the SES activities agree favorably with the theoretical estimation of Eq. (A2).

The latter fact, i.e., that the SES activities exhibit a behavior compatible with a model based on the random-field Ising Hamiltonian at the critical point, while the  $\kappa_1$  value that reproduces the ICFMC data ( $=0.080 \pm 0.003$ ) exceeds (slightly, but by an amount larger than the experimental error) the aforementioned one (i.e.,  $\kappa_1=0.070$ ), which resulted from Eq. (A2), is currently under detailed investigation.

- 
- [1] H.E. Stanley, *Introduction to Phase Transitions and Critical Phenomena* (Oxford University Press, London, 1971).
- [2] H.E. Stanley, *Rev. Mod. Phys.* **71**, S358 (1999).
- [3] S.V. Buldyrev, N.V. Dokholyan, A.L. Goldberger, S. Havlin, C.-K. Peng, H.E. Stanley, and G.M. Viswanathan, *Physica A* **249**, 430 (1998).
- [4] G.M. Viswanathan, S.V. Buldyrev, S. Havlin, and H.E. Stanley, *Physica A* **249**, 581 (1998).
- [5] G.H. Weiss, *Random Walks* (North-Holland, Amsterdam, 1994).
- [6] P. Varotsos and K. Alexopoulos, *Thermodynamics of Point Defects and their Relation with Bulk Properties* (North-Holland, Amsterdam, 1986).
- [7] C.-K. Peng, S.V. Buldyrev, S. Havlin, M. Simons, H.E. Stanley, and A.L. Goldberger, *Phys. Rev. E* **49**, 1685 (1994).
- [8] S.V. Buldyrev, A.L. Goldberger, S. Havlin, R.N. Mantegna, M.E. Matsa, C.-K. Peng, M. Simons, and H.E. Stanley, *Phys. Rev. E* **51**, 5084 (1995).
- [9] P. Varotsos, K. Alexopoulos, K. Nomicos, and M. Lazaridou, *Nature (London)* **322**, 120 (1986).
- [10] P. Varotsos, M. Lazaridou, K. Eftaxias, G. Antonopoulos, J. Makris, and J. Kopanas, in *The Critical Review of VAN: Earthquake Prediction from Seismic Electric Signals*, edited by Sir J. Lighthill (World Scientific, Singapore, 1996), p. 29.
- [11] S. Uyeda, T. Nagao, Y. Orihara, T. Yamaguchi, and I. Takahashi, *Proc. Natl. Acad. Sci. U.S.A.* **97**, 4561 (2000).
- [12] P. Varotsos, *Acta Geophys. Pol.* **49**, 1 (2001).
- [13] P. Varotsos, N. Sarlis, and E. Skordas, *Proc. Jpn. Acad., Ser. B: Phys. Biol. Sci.* **77**, 93 (2001).
- [14] H.E. Hurst, *Trans. Am. Soc. Civ. Eng.* **116**, 770 (1951).
- [15] J. Bassingthwaighte, L.S. Liebovitch, and B.J. West, *Fractal Physiology* (Oxford University Press, Oxford, 1994).
- [16] R.M. Dünki and B. Ambühl, *Physica A* **230**, 544 (1996).
- [17] Z.-G. Yu, V.V. Anh, and B. Wang, *Phys. Rev. E* **63**, 011903 (2000).
- [18] S. Mercik and K. Weron, *Phys. Rev. E* **63**, 051910 (2001).
- [19] A. Fuliński, Z. Grzywna, I. Mellor, Z. Siwy, and P.N.R. Usherwood, *Phys. Rev. E* **58**, 919 (1998).
- [20] A. Fuliński, *Phys. Rev. Lett.* **79**, 4926 (1997).
- [21] P. Varotsos, *The Physics of Seismic Electric Signals* (TERRA-PUB, Tokyo, in press).

- [22] P. Varotsos, N. Sarlis, and E. Skordas, *Practica of the Athens Academy* **76**, 388 (2001).
- [23] K. Weron and S. Mercik, (private communication).
- [24] P. Talkner and R.O. Weber, *Phys. Rev. E* **62**, 150 (2000).
- [25] A.L. Goldberger, L.A.N. Amaral, L. Glass, J.M. Hausdorff, P.C. Ivanov, R.G. Mark, J.E. Mietus, G.B. Moody, C.-K. Peng, and H.E. Stanley, *Physionet*, <http://circ.ahajournals.org/cgi/content/full/101/23/e215> 2000.
- [26] Z. Siwy, M. Ausloos, and K. Ivanova, *Phys. Rev. E* **65**, 0311907 (2002).
- [27] T. Antal, M. Droz, G. Györgyi, and Z. Rácz, *Phys. Rev. E* **65**, 046140 (2002).
- [28] R.M. Dünki, E. Keller, P.F. Meier, and B. Ambühl, *Physica A* **276**, 596 (2000).
- [29] P. Varotsos, N. Sarlis, and E. Skordas, *Acta Geophys. Pol.* **49**, 425 (2001).
- [30] S. Mercik, K. Weron, and Z. Siwy, *Phys. Rev. E* **60**, 7343 (1999).
- [31] Z. Siwy, S. Mercik, K. Weron, and M. Ausloos, *Physica A* **297**, 79 (2001).
- [32] L.P. Kadanoff, *Statistical Physics, Statics, Dynamics and Renormalization* (World Scientific, Singapore, 2000).
- [33] E. Manousakis and R. Salvador, *Phys. Rev. B* **40**, 2205 (1989).
- [34] P. Varotsos, N. Sarlis, and M. Lazaridou, *Phys. Rev. B* **59**, 24 (1999).
- [35] E.V. Russell and N.E. Israeloff, *Nature (London)* **408**, 695 (2000).
- [36] A.K. Jonscher, *Universal Relaxation Law* (Chelsea Dielectric Press, London, 1996).
- [37] A.S. Nowick, A.V. Vaysleyb, and I. Kuskovsky, *Phys. Rev. B* **58**, 8398 (1998).
- [38] K. Weron, A. Jurlewicz, and A.K. Jonscher, *IEEE Trans. Dielectr. Electr. Insul.* **8**, 352 (2001).
- [39] C. Zey, STATISTICAL METHODS GROUP, NIST, and SEMATECH, NIST-SEMATECH, [www.itl.nist.gov/div898/handbook](http://www.itl.nist.gov/div898/handbook), 2000.
- [40] M.C. Kuntz and J.P. Sethna, *Phys. Rev. B* **62**, 11 699 (2000).